

# Dynamic Loss For Robust Learning

Shenwang Jiang<sup>†</sup> Jianan Li<sup>\*†</sup> Jizhou Zhang Ying Wang Tingfa Xu<sup>\*</sup>

Beijing Institute of Technology

## Abstract

Label noise and class imbalance commonly coexist in real-world data. Previous works for robust learning, however, usually address either one type of the data biases and underperform when facing them both. To mitigate this gap, this work presents a novel meta-learning based dynamic loss that automatically adjusts the objective functions with the training process to robustly learn a classifier from long-tailed noisy data. Concretely, our dynamic loss comprises a label corrector and a margin generator, which respectively correct noisy labels and generate additive per-class classification margins by perceiving the underlying data distribution as well as the learning state of the classifier. Equipped with a new hierarchical sampling strategy that enriches a small amount of unbiased metadata with diverse and hard samples, the two components in the dynamic loss are optimized jointly through meta-learning and cultivate the classifier to well adapt to clean and balanced test data. Extensive experiments show our method achieves state-of-the-art accuracy on multiple real-world and synthetic datasets with various types of data biases, including CIFAR-10/100, Animal-10N, ImageNet-LT, and Webvision. Code will soon be publicly available.

Deep neural networks (DNNs) have reached great success owing to the rapid growth of labeled data. Most real-world data, however, comes with both long-tailed distributions and inevitable noisy labels. Such biased data make DNNs easily neglect tail classes (Cao et al. 2019), memorize noisy training labels (Jiang et al. 2018), and thus under-perform on balanced clean test data. Recently, the issue of robust learning from long-tailed data with noisy labels is attracting increasing attention (Jiang et al. 2022; Cao et al. 2020).

Among recent advances in robust learning (Shu et al. 2019; Jiang et al. 2018; Kang et al. 2019; Liu et al. 2019), correcting noisy labels (Li, Socher, and Hoi 2020) and adjusting classification margins (Cao et al. 2019) are two advanced practices to tackle label noise and class imbalance, respectively. These solutions, however, largely rely on manually-designed rules to divide noisy and clean samples, or pre-set parameters to obtain prior knowledge of class distribution. Such manual interventions are impractical when label noise meets class imbalance, since tail classes make it difficult to recognize label noise while the presence of noisy labels in turn makes observed class distribution unreliable.

<sup>\*</sup>Corresponding author, <sup>†</sup> represents equal contributions

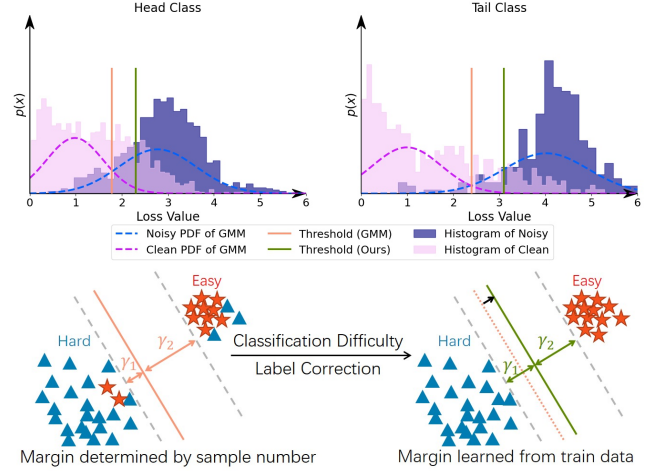


Figure 1: **Upper:** Conventional class-specific GMM with fixed hyperparameters tends to divide clean samples into the noisy split, while our label corrector learns the optimal division thresholds on different classes from train data and samples’ class-specific loss rank. **Lower:** Previous methods generate classification margin  $\gamma$  based solely on the sample number. In contrast, our margin generator respects the presence of noisy labels and the distinct classification difficulties of different classes, leading to a more appropriate margin.

Hence, we are dedicated to paving a new way for robust learning from biased data in a fully self-adaptive manner.

With the above in mind, we present a novel meta-learning based dynamic loss, comprised of a learnable *label corrector* and a *margin generator*, to learn a classifier robustly from long-tailed noisy data. In contrast to predefined fixed objective functions adopted by priors, our dynamic loss learns to simultaneously correct per-sample labels and adjust per-class classification margins by perceiving the underlying data distribution and the learning state of the classifier, hence providing suitable dynamic learning objectives with the training process.

For correcting noisy labels, the key challenge is how to identify noisy samples and ignore or reuse them. Previous solutions usually use a GMM with fixed-hyperparameters to distinguish between noisy and clean samples based on their loss values, which fails on long-tailed noisy data since

some clean samples of tail classes may have even higher loss values than noisy samples of head classes due to highly skewed class distribution. A straightforward solution is to design a class-specific GMM (Huang et al. 2022), which still tends to be confused due to the dramatically different noise rates among different classes (Figure 1). Moreover, previous methods relabel identified noisy samples by fusing their assigned labels and classifier’s predictions in a fixed manner. Since the classifier is inaccurate at the start of training and prone to overfitting to noisy samples at the end, blindly trusting classifier’s predictions throughout the training easily causes incorrect corrections. To tackle the above issues, we design a novel label corrector that learns to jointly identify and relabel noisy samples in a fully learnable fashion by respecting both the class-specific loss rank of samples and the learning state of the classifier.

For adjusting per-class classification margins, we are motivated by the fact that classes with fewer samples have larger generalization error bounds, which can be minimized by increasing the classification margin (Cao et al. 2019). Most priors (Ren et al. 2020) pre-define a fixed margin for each class based solely on its sample number (Figure 1). They suffer two drawbacks: i) the per-class sample number becomes unreliable in the presence of noisy labels; ii) the distinct classification difficulties among different classes have been simply ignored. To mitigate this, we develop a novel margin generator that learns to generate a suitable dynamic margin for each class by self-perceiving the true class distribution underlying the noisy data as well as the classification difficulty of each class.

We integrate the label corrector and the margin generator into a unified dynamic loss and optimize them through meta-learning, such that the objective function for the classifier can be dynamically adjusted throughout the training. To collect a small amount of unbiased meta data, we design a new hierarchical sampling strategy that first builds a random primary set and then a balanced clean meta set progressively. This enables the built meta set enriched with diverse and hard samples to better simulate the distribution of real test data, hence avoiding biased learning on too much easy samples. Consequently, our dynamic loss is capable of guiding the classifier learning robustly on various types of biased data in a fully self-adaptive manner.

We comprehensively evaluate our dynamic loss on both synthetic and real-world long-tailed data with label noise. It achieves state-of-the-art results on a wide variety of benchmarks with various imbalance ratios and noise rates, including CIFAR-10/100 (Krizhevsky, Hinton et al. 2009), Animal-10N (Song, Kim, and Lee 2019), ImageNet-LT (Liu et al. 2019) and Webvision (Li et al. 2017). Additional tests on purely imbalanced or noisy data further validate its great adaptability and robustness.

To sum up, this work makes the following contributions:

- We propose a simple yet effective dynamic loss, which paves a new way for robust learning on various biased data in a fully self-adaptive manner.
- We present a novel hierarchical sampling strategy to effectively construct unbiased yet diverse meta data.

- We establish new state-of-the-arts on multiple synthetic and real-world datasets.

## Related Works

**Long-Tailed Learning.** Existing methods of long-tailed learning are generally divided into three categories: data re-sampling (Chawla et al. 2002; Buda, Maki, and Mazurowski 2018), adjusting the classification boundary (Tang, Huang, and Zhang 2020), and re-weighting (Shu et al. 2019; Lin et al. 2017; Huang et al. 2016). The re-sampling’s idea is to rebalance the class distribution by over-sampling the tail classes, which is effective but prone to overfitting on the tail classes. Methods of the second category enlarges the classification boundary of the tail classes while narrowing that of the head classes, by modifying the classification threshold (Menon et al. 2020), or by adjusting the weights of the output layer through normalization (Kang et al. 2019). The re-weighting strategy aims to assign larger loss weights to the tail classes. Conventional approaches of this category (Huang et al. 2016, 2019a) directly impose weights on each training sample, which is sensitive to outliers and causes unstable training (Ren et al. 2020). Some recent works (Tan et al. 2020) achieve re-weighting by modifying the predicted scores in the Softmax function, which yields more stable training and promising performance. This work inherits the merit of re-weighting strategy by adapting it to more challenging long-tailed scenarios with label noise.

**Learning under Label Noise.** Methods of learning under label noise can be categorized into two main types: sample re-weighting and relabeling. The re-weighting strategy treats samples with larger loss values as noise, and reduce their influence by giving them lower weights (Kumar, Packer, and Koller 2010; Huang et al. 2019b). MentorNet (Jiang et al. 2018) learns data-driven curriculums for deep CNNs trained on corrupted labels. Meta-Weight-Net (Shu et al. 2019) learns an explicit weighting function directly from a small clean data set. The relabeling strategy leverages noisy samples by refining their labels. Bootstrapping (Reed et al. 2014) integrates assigned labels and model’s predictions by interpolation. Some works divide clean and noisy samples based on the priors learned from a manually generated noisy set (Chen, Zhu, and Chen 2021), and then take advantage of noisy samples (Berthelot et al. 2019).

**Long-tailed Learning under Label Noise.** Recently, some works have emerged to cope with long-tailed learning under label noise. HAR (Cao et al. 2020) regularizes different regions of the input space differently through data-dependent regularization technique. CurveNet (Jiang et al. 2022) learns to assign proper weights to different samples according to sample’s loss curve. ROLT (Wei et al. 2021) combines DivideMix and LDAM to correct noisy labels and improve tail-class performance. Different from these methods, this work makes the first trial to correct noisy labels and adjust per-class classification margin simultaneously in a learnable and adaptive manner according to the training data.

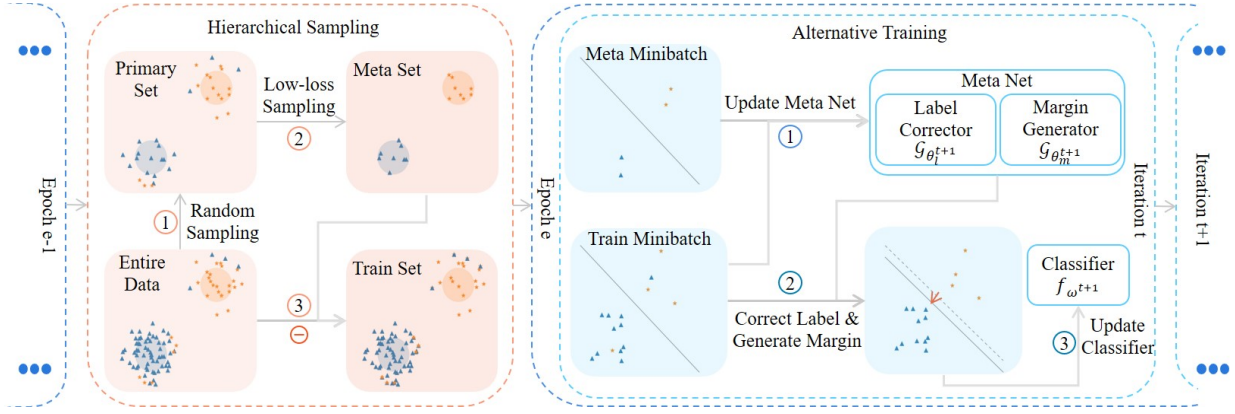


Figure 2: Overall learning paradigm with our dynamic loss. Each training epoch begins with dividing the entire data into a small unbiased meta set and a biased train set. At each iteration, we first update the label corrector and the margin generator jointly through meta-learning on mini-batch meta and train data; then the classifier is updated on mini-batch train data by minimizing the dynamic loss with corrected per-sample labels and generated per-class margins.

## Methods

This section describes the details of our dynamic loss and its optimization through meta-learning.

### Overview

Given a noisy and imbalanced train set  $\mathcal{D} = \{\mathbf{x}_i, \mathbf{y}_i\}_{i=1}^N$  with image  $\mathbf{x}_i$  and its assigned one-hot class label  $\mathbf{y}_i$ , our goal is to learn a classifier  $\mathbf{f}_\omega$  with learnable parameters  $\omega$  that maps an input image to class confidence scores. Despite of the label noise and class imbalance existed in the train set, the classifier is required to accurately recognizing all classes, so a balanced and clean test set is employed.

The parameters  $\omega$  are optimized by minimizing the classification loss on the train set:

$$\omega^* = \arg \min_{\omega} \sum_{i=1}^N \ell(\mathbf{y}_i, \mathbf{f}_\omega(\mathbf{x}_i)). \quad (1)$$

where  $\ell(\cdot)$  is the cross-entropy loss. Since the train set is with both label noise and class imbalance, optimizing with such naive cross-entropy loss suffers two major drawbacks: i) the assigned labels of noisy samples do not match their ground-truths, which result in high loss values and force the model to memorize noisy labels; ii) tail classes have much lower occurrence probabilities but share the same classification margins as that of head classes and thus are prone to poor generalization.

To tackle the above two problems, we present a novel dynamic loss that simultaneously corrects noisy labels and adjusts the classification margin for different classes in an adaptive and learnable manner:

$$\mathcal{DL} = \ell(\mathbf{y}_i^*, \mathbf{f}_\omega(\mathbf{x}_i) + \mathbf{q}), \quad (2)$$

where  $\mathbf{y}_i^*$  and  $\mathbf{q} \in \mathbb{R}^C$  denote the reassigned label and the additive classification margin for  $\mathbf{x}_i$ , respectively.

Concretely, as illustrated in Figure 2, the dynamic loss is equipped with a learnable label corrector  $\mathcal{G}_{\theta_l}$  parameterized by  $\theta_l$  and a margin generator  $\mathcal{G}_{\theta_m}$  parameterized by  $\theta_m$ , which are respectively in charge of correcting per-sample labels and per-class classification margins. We continuously

optimize them jointly along with the classifier  $\mathbf{f}_\omega$  through meta-learning. Next, we describe the two counterparts as well as their optimization in detail.

### Label Corrector

The label corrector identifies noisy samples and corrects their wrongly assigned labels in a class-wise manner. For identifying noisy samples, it divides all samples into  $C$  groups by class and sorts the samples in each group separately according to the loss value, evenly divides the sorted samples in each group into  $R$  bins, and employs a lightweight class-wise meta net to learn to identify whether the bin  $r \in \{1, \dots, R\}$  is dominated by noisy or clean samples. Consequently, the loss bin index  $r_i$  for sample  $i$  can server as a reliable indicator for identifying label noise.

For label correction, as long as the classifier has not severely over-fitted on biased data, it learns mainly from the dominated clean samples and transfers the learned knowledge to noisy ones. Hence, the classifier’s predictions on noisy samples are close to their ground-truths and can be used to correct the wrongly assigned labels.

Based on the above, here comes our label corrector that reassigns a ground-truth label  $\mathbf{y}_i^*$  for sample  $\mathbf{x}_i$  as a weighted sum of its assigned label  $\mathbf{y}_i$  and the classifier’s prediction  $\mathbf{y}'_i$  based on the loss bin index  $r_i$ :

$$\begin{aligned} \mathbf{y}_i^* &= \mathcal{G}_{\theta_l}(\mathbf{y}_i, \mathbf{y}'_i, r_i) \\ &= \mathbf{y}_i * g(r_i | \mathbf{y}_i) + \mathbf{y}'_i * (1 - g(r_i | \mathbf{y}_i)), \end{aligned} \quad (3)$$

where  $g : r_i | \mathbf{y}_i \rightarrow [0, 1]$  is a class-dependent weighting function that maps the bin index  $r_i$  to a balance weight. It is learned by a small meta net, implemented by a one-hot encoder followed by a two-layer perceptron (MLP) with sibling Sigmoid activation. If sample  $i$  is noisy with a high loss value,  $r_i$  is large and the computed  $g(r_i | \mathbf{y}_i)$  is close to 0, hence the label corrector corrects its wrongly assigned label with the classifier’s prediction, and vice versa.

### Margin Generator

For the design of the margin generator, we begin with revisiting Label-Distribution-Aware Margin Loss (LDAM) from

the perspective of generalization error bound. Due to fewer training samples, tail classes have larger generalization error bounds compared with head classes. Since the generalization error bound usually negatively correlates to the magnitude of classification margin, increasing the classification margins for the tail classes will minimize their generalization error bounds.

In light of the above, Balanced Meta-Softmax, an unbiased extension of standard Softmax, adjusts the classification margin for class  $j$  based on its sample number  $n_j$ , and poses the additive margin  $-\log(n_j)$  to the confidence score  $p_j$  predicted by the classifier:

$$\ell'(\omega|y=j) = -\log\left(\frac{e^{p_j+\log(n_j)}}{\sum_{i=1}^C e^{p_i+\log(n_i)}}\right). \quad (4)$$

However, for long-tailed data with noisy labels,  $n_j$  can no longer reflect the real sample number of class  $j$  due to the existence of label noise. In addition, manually pre-defining the margin based solely on the sample number largely ignores the distinct classification difficulties of different classes.

We hence present a learnable margin generator  $\mathcal{G}_{\theta_m}$ , implemented by a two-layer MLP, to dynamically adjust the margin for each class by optimizing a learnable margin vector  $\mathbf{q} \in \mathbb{R}^C$  from an initial all-ones vector during classifier training:

$$\mathbf{q} = \mathcal{G}_{\theta_m}(\mathbf{1}) = [q_1, \dots, q_C]. \quad (5)$$

By integrating the margin vector into the standard Softmax loss, we have:

$$\hat{\ell}(\omega|y=j) = -\log\left(\frac{e^{p_j+q_j}}{\sum_{i=1}^C e^{p_i+q_i}}\right). \quad (6)$$

Since the classification margin is  $-q_j$  in our formulation, the learned margin  $q_j$  for class  $j$  should be positively correlated to its sample number.

Hence the margin generator is capable of adjusting per-class margins automatically by adapting to the true class distribution underlying the long-tailed noisy data and the classification difficulty of each class in a learnable manner, with no manual interventions nor prior information required.

## Hierarchical Sampling Strategy

We integrate the label corrector  $\mathcal{G}_{\theta_l}$  and the margin generator  $\mathcal{G}_{\theta_m}$  into a unified meta net  $\mathcal{G}_{\theta}$ , the key component of our dynamic loss. We apply meta-learning to optimize  $\mathcal{G}_{\theta}$  and guide the learning of the classifier  $\mathbf{f}_{\omega}$  to well adapt to balanced and clean test data.

Performing meta-learning requires to build a meta set  $\mathcal{D}_c = \{(\mathbf{x}_i, \mathbf{y}_i)\}_{i=1}^M$  comprised of a small amount of balanced and clean data. Intuitively, samples with lower classification loss computed by  $\mathbf{f}_{\omega}$  tend to have correctly assigned labels. Hence we can build the meta set simply by selecting  $M_1$  samples with the lowest loss values from each class in  $\mathcal{D}$ . However, since easier samples usually have lower loss values throughout the training, such a sampling strategy tend to select fixed easy samples at each epoch, making the model prone to overfitting to easy samples.

Hereby, we design a hierarchical sampling strategy to build  $\mathcal{D}_c$  through a two-step process: i) construct a *primary set* by randomly sampling  $M_0$  samples from each class in  $\mathcal{D}$ ; ii) select  $M_1$  low-loss samples from each class in the *primary set* to form the final meta set. The remaining samples in  $\mathcal{D}$  make up the counterpart set  $\mathcal{D}_n$ , as illustrated in Fig. 2.

The benefits of introducing the additional primary set are twofold: i) the samples in the primary set are randomly sampled at each epoch, which guarantees the resulting meta set to be distinct across different epochs; ii) the primary set has fewer samples than  $\mathcal{D}$ , which enables a larger probability of selecting hard yet clean samples near the decision boundary into the meta set. As a result, our hierarchical sampling strategy ensures both the dynamism and diversity of the meta set, preventing the model from overfitting to biased data.

## Optimization

$\theta^t$  and  $\omega^t$  respectively denote the parameters of the meta net and the classifier at iteration  $t$ . We randomly sample two mini-batches  $\mathcal{X}_c$  and  $\mathcal{X}_n$  from  $\mathcal{D}_c$  and  $\mathcal{D}_n$ , respectively, and update  $\theta^t$  and  $\omega^t$  alternatively as follows.

*Update  $\theta^t$ .* The meta net  $\mathcal{G}_{\theta^t}$  is trained to guide the learning of the classifier  $\mathbf{f}_{\omega^t}$  on  $\mathcal{X}_n$  by correcting per-sample labels and adjusting per-class margins, such that  $\mathbf{f}_{\omega^t}$  can well adapt to the balanced and clean  $\mathcal{X}_c$ . We first virtually update  $\omega^t$  on the dynamic loss with  $\mathcal{G}_{\theta^t}$ :

$$\hat{\omega}^t = \omega^t - \alpha \frac{1}{m_0} \sum_{(\mathbf{x}_i, \mathbf{y}_i) \in \mathcal{X}_n} \nabla_{\omega} \mathcal{D}\mathcal{L}(\mathbf{x}_i, \mathbf{y}_i; \theta^t, \omega) |_{\omega^t}, \quad (7)$$

where  $\alpha$  is the learning rate for the classifier and  $m_0$  is the batch size. Then we update  $\theta^t$  by minimizing the loss of the virtually updated classifier  $\mathbf{f}_{\hat{\omega}^t}$  on  $\mathcal{X}_c$ :

$$\theta^{t+1} = \theta^t - \beta \frac{1}{m_0} \sum_{(\mathbf{x}_i, \mathbf{y}_i) \in \mathcal{X}_c} \nabla_{\theta} \ell(\mathbf{x}_i, \mathbf{y}_i; \hat{\omega}^t) |_{\theta^t}. \quad (8)$$

where  $\beta$  is the learning rate for the meta net.

*Update  $\omega^t$ .* We update  $\omega^t$  by minimizing the loss of  $\mathbf{f}_{\omega^t}$  on  $\mathcal{X}^n$  with corrected labels and adjusted margins by the updated  $\mathcal{G}_{\theta^{t+1}}$ :

$$\omega^{t+1} = \omega^t - \alpha \frac{1}{m_0} \sum_{(\mathbf{x}_i, \mathbf{y}_i) \in \mathcal{X}_n} \nabla_{\omega} \mathcal{D}\mathcal{L}(\mathbf{x}_i, \mathbf{y}_i; \theta^{t+1}, \omega) |_{\omega^t}. \quad (9)$$

The above two steps are repeated over iterations so that  $\mathcal{G}_{\theta}$  and  $\mathbf{f}_{\omega}$  are optimized alternatively until convergence.

## Experiments

We test our method on both synthetic and real-world long-tailed noisy data, and then present ablations to validate our design choices. More quantitative and qualitative results and training details are provided in supplementary materials.

**Methods in Comparison.** We compare with three types of methods that are respectively designed to address: i) both label noise and class imbalance, such as HAR, ROLT, FAMUS (Xu et al. 2021) and CurveNet; ii) label noise, such as Co-teaching (Han et al. 2018), SELFIE (Song, Kim, and Lee 2019), DivideMix, ELR+ (Liu et al. 2020), NCT (Chen

Methods	CIFAR-10-N-LT		CIFAR-100-N-LT		WebVision		ImageNet	
	Last	Best	Last	Best	Top-1	Top-5	Top-1	Top-5
Cross Entropy	52.73	60.43	25.41	26.67	71.08	88.48	65.08	87.48
DivideMix	58.19	60.74	41.15	41.75	77.32	91.64	75.20	90.84
Balanced-Softmax	69.66	76.37	41.30	41.82	63.48	84.56	61.80	85.32
DivideMix+Balanced-Softmax	71.60	72.75	46.11	46.92	78.76	92.52	76.60	92.76
CurveNet	69.36	71.36	29.83	32.72	-	-	-	-
HAR	76.52	77.17	42.77	43.98	75.50	90.70	70.30	90.00
ROLT+	75.31	-	38.94	-	77.64	92.44	74.64	92.48
ELR+	69.31	70.34	34.96	36.20	77.78	91.68	70.29	89.76
FaMUS	39.12	46.98	30.72	30.81	79.40	92.80	<b>77.00</b>	92.76
<b>Dynamic Loss (Ours)</b>	<b>79.73</b>	<b>80.55</b>	<b>48.56</b>	<b>48.98</b>	<b>80.12</b>	<b>93.64</b>	74.76	<b>93.08</b>

Table 1: Accuracy (%) on CIFAR-N-LT, WebVision, and ImageNet.

et al. 2022), PLC (Zhang et al. 2021), GJS (Engleson and Azizpour 2021), and CMW-Net (Shu et al. 2022); and iii) class imbalance, such as Focal Loss, CB focal (Cui et al. 2019), LDAM and Balanced Softmax.

## Experiments on Long-Tailed Noisy Data

**Results on CIFAR-N-LT.** We evaluate our method on CIFAR-N-LT including CIFAR-10 and CIFAR-100 with simulated label noise and class imbalance. We first simulate the long-tailed dataset by following the exponential profile (Cao et al. 2019), with imbalance ratio  $\rho$ . The long-tailed imbalance follows an exponential decay in the sample number across different classes. We then inject label noise to the long-tailed dataset to form the training set. In particular, the label of each sample is independently changed to class  $j$  with probability  $\frac{N_j}{N}\lambda$ , where  $N$  is the total number of training samples and  $N_j$  denotes the frequency of class  $j$ . Following ROLT, we consider the imbalance ratio of  $\rho \in \{10, 100\}$  and the noise rate of  $\lambda \in \{0.1, 0.2, 0.3, 0.4, 0.5\}$ . We adopt the ResNet-32 (He et al. 2016a) as the classifier.

Table 1 depicts the average accuracy on CIFAR-10 and CIFAR-100 with various imbalance ratios and noise rates, respectively. Our method retains high accuracy under a wide range of degrees for both biases, while previous methods degrade rapidly. In particular, our dynamic loss improves the average last accuracy by 4.03% and 5.79% compared to HAR on CIFAR-10-N-LT and CIFAR-100-N-LT, respectively. Moreover, it significantly outperforms the baseline model that simply fuses strategies from DivideMix and Balanced-Softmax.

It is worth mentioning that previous methods rely on carefully tuned hyper-parameters based on unobservable noise rate (Li, Socher, and Hoi 2020) or perform two-stage training to get prior information of class distribution (Cao et al. 2020). In comparison, our dynamic loss uses a fixed set of hyper-parameters and requires only one-round end-to-end training without any manual interventions in all the experiments.

**Results on Webvision.** We also evaluate our dynamic loss

Methods	CIFAR-10-N	CIFAR-100-N	Animal-10N
Cross Entropy	79.92	46.37	80.60
SELFIE	-	50.23	81.80
PLC	79.79	47.36	83.40
NCT	87.95	56.88	84.10
Co-teaching	85.45	58.34	80.20
CMW-Net	89.41	64.29	84.70
DivdeMix	94.11	73.77	84.00
GJS	90.94	70.52	84.17
<b>Dynamic Loss</b>	<b>94.62</b>	<b>74.24</b>	<b>86.54</b>

Table 2: Accuracy (%) on CIFAR-N and Animal-10N.

on WebVision, a real-word long-tailed noisy dataset. We adopt Inception-ResNet V2 (Szegedy et al. 2017) as the classifier by following priors (Li, Socher, and Hoi 2020). Table 1 shows the results on WebVision and ImageNet (Deng et al. 2009) validation set. Our method significantly outperforms other competing methods despite most of them are equipped with additional model cotraining and ensembling strategies. Notably, compared to HAR and ROLT+ that are dedicated to dealing with long-tailed noisy data, our method boosts the accuracy by at least 2.48% on WebVision, which clearly demonstrates its superiority.

## Experiments on Noisy Data

**Results on CIFAR-N.** We test the performance of our dynamic loss in dealing with purely noisy data on CIFAR-10-N and CIFAR-100-N with symmetric noise rates  $\{0.2, 0.4, 0.6\}$  and asymmetric noise rates  $\{0.2, 0.4\}$ . We adopt PreAct ResNet (PARes18) (He et al. 2016b) as the classifier by following DivideMix. Table 2 depicts our method achieves the best average accuracy compared to previous methods specially designed for learning on noisy data. In contrast to DivideMix that requires to manually tune the



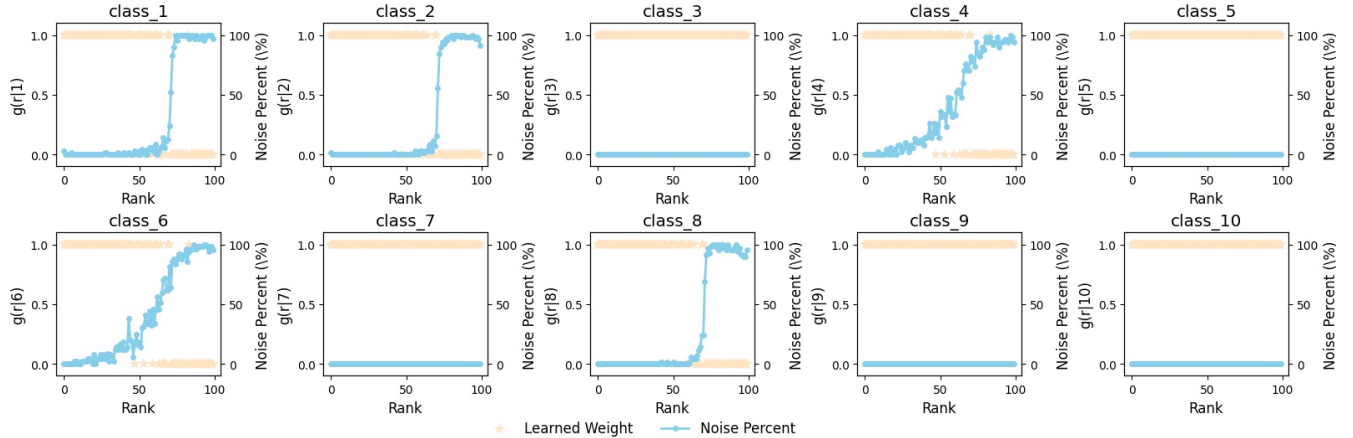


Figure 3: Visualizing the learned label weights  $g(r|y)$  and noise percentage for each class on CIFAR-10-N (Asym.  $\lambda = 0.4$ ).

hyper-parameters under different noise types and rates, our dynamic loss well adapts to various noisy scenarios in a fully self-adaptive manner without manual interventions.

**Results on Animal-10N.** We also test on Animal-10N real-world noisy dataset. For a fair comparison with priors (Song, Kim, and Lee 2019), we adopt randomly initialized VGG19-BN (Simonyan and Zisserman 2015) as the classifier. Table 2 shows our dynamic loss achieves state-of-the-art performance among all priors, which clearly proves its superiority in dealing with real-world noisy data.

### Experiments on Long-Tailed Data

**Results on CIFAR-LT.** We also test the performance of our dynamic loss in dealing with purely long-tailed data on clean CIFAR datasets with varying imbalance ratios  $\rho \in \{10, 20, 50, 100\}$ . Table 3 depicts our method achieves the best performance compared to previous methods specially designed for learning on long-tailed data. Especially, compared with LDAM that adjusts classification margins based solely on the sample number, our method significantly boosts the accuracy by 4.03% and 5.75% on CIFAR-10-LT and CIFAR-100-LT, respectively. It evidences that our dynamic loss is capable of perceiving the classification difficulty of different classes and adjusting their classification margins adaptively.

**Results on ImageNet-LT.** Table 3 reports the results on ImageNet-LT, a large-scale long-tailed dataset with imbalance ratio  $\rho = 256$ . Our dynamic loss achieves the best performance, *i.e.*, 38.39% in accuracy, demonstrating its strong generalization ability.

### Qualitative Analysis.

**Behavior of label corrector.** We analyze the behavior of the label corrector on balanced CIFAR-10-N with asymmetric noise that is designed to mimic the structure of real-world label noise by assigning distinct noise rates to different classes. Figure 3 depicts the learned weight  $g(r|y)$  by the label corrector and the percentage of noisy labels corresponding to increasing loss bin index  $r$  on each class. For the classes that contain noisy labels, clean samples mainly

Methods	CIFAR-10-LT	CIFAR-100-LT	ImageNet-LT
Cross Entropy	78.45	47.26	34.01
Focal Loss	79.13	47.62	32.64
CB Focal	81.42	48.88	-
LDAM-DRW	83.21	51.36	36.03
FaMUS	84.61	52.73	-
Balanced-Softmax	87.15	57.08	38.21
<b>Dynamic Loss</b>	<b>87.24</b>	<b>57.11</b>	<b>38.39</b>

Table 3: Accuracy (%) on CIFAR-LT and ImageNet-LT.

appear at top-ranked (low-loss) bins while noisy samples at bottom-ranked (high-loss) bins. This validates our motivation that the loss bin index  $r$  can serve as a reliable input indicator for the label corrector to distinguish between noisy and clean samples. Accordingly, the generated weight  $g(r|y)$  remains to be 1 and suddenly drops to 0 at around bin 60, showing that the label corrector retains the assigned ground-truth label for clean samples and turns to the predicted label that is more likely to be the ground-truth for noisy samples. While for the classes without noisy labels,  $g(r|y)$  remains to be 1. Consequently, our label corrector always outputs the correct labels for both noisy and clean samples of different classes.

**Behavior of margin generator.** We analyze the behavior of the margin generator on clean CIFAR-10-LT with imbalance factor  $\rho = 20$ . We visualize its generated margins for different classes in the left subfigure of Figure 4. Generally, as the class index increases, the sample number decreases, and the learned margin also decreases as expected. It suggests that the margin generator automatically figures out the sample number of different classes and adjusts their margins accordingly. Interestingly, we see some irregularly larger margins on class 9 and 10. This can be explained by the right subfigure in which we visualize the feature distribution of meta set using T-SNE (Van der Maaten and Hinton 2008). The feature distribution of these two classes correspond to the two rightmost clusters, indicating they are easier to be distinguished

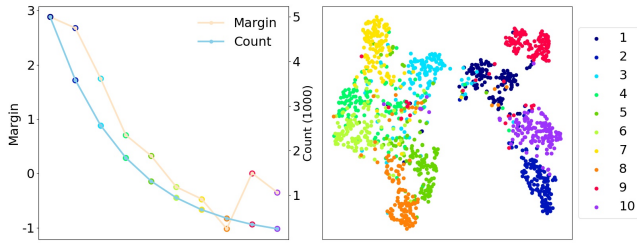


Figure 4: Visualization of learned per-class margins and samples number (left), and samples' feature distribution of meta set (right) on CIFAR-10-LT ( $\rho = 20$ ).

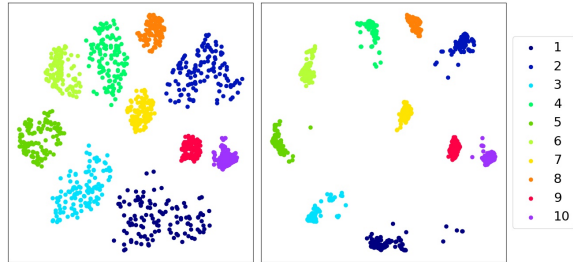


Figure 5: Visualization of samples' feature distribution of the meta set constructed by hierarchical sampling (left), and by naive sampling (right) on CIFAR-10-N-LT ( $\rho = 10$  and  $\lambda = 0.2$ ).

from the other classes. This evidences that the margin generator takes into account not only the sample number, but also the classification difficulty of each class, to generate comprehensively adaptive margins during classifier training.

**Behavior of hierarchical sampling.** We investigate how our hierarchical sampling strategy improves meta set construction. Figure 5 illustrates samples' feature distribution of the meta set built by our hierarchical sampling (left) and by naive sampling (right). Compared with naive sampling, the feature distribution of samples selected by hierarchical sampling are more spread out within separate clusters. It evidences that building a primary set prior to random sampling enables more diverse meta data covering both easy and hard samples, and thus alleviates biased learning on easy samples.

## Ablation Studies.

**Effect of label corrector.** We build a model variant in which the label corrector is excluded to evaluate its effectiveness. Table 4 depicts its average accuracy decreases by 8.26% compared with complete dynamic loss, which well evidences the effectiveness of the label corrector.

**Effect of margin generator.** As shown in Table 4, to verify the effectiveness of the margin generator, we firstly only employ the label corrector, which achieves the average last accuracy of 71.08%. Thereafter, we introduce Balanced-Softmax to deal with class imbalance, which only lifts a little accuracy by 1.56%. Finally, we boost the accuracy to 79.77% by equipping our margin generator. These evidence a dynamic margin is necessary to long-tailed noisy data.

**Effect of hierarchical sampling.** As shown in Table 4, replacing the hierarchical sampling with naive random sampling results in up to 1.24% average last accuracy drop,

$\mathcal{G}_{\theta_l}$	$\mathcal{G}_{\theta_m}$	B	H	V	Last	Best
					52.73	60.43
	✓		✓		71.51	76.84
✓			✓		71.08	77.11
✓		✓	✓		72.64	74.96
✓	✓				78.53	79.58
✓	✓		✓	✓	79.50	80.35
✓	✓		✓		<b>79.77</b>	<b>80.55</b>

Table 4: Ablations. B: Balanced-Softmax, H: hierarchical sampling, and V: vector meta net.

Methods	CIFAR-10		CIFAR-100	
	Last	Best	Last	Best
HAR	71.09	71.63	39.35	39.86
<b>Dynamic Loss</b>	<b>79.99</b>	<b>82.20</b>	<b>41.15</b>	<b>41.73</b>

Table 5: Mean accuracy (%) of PAREs18 on CIFAR-N-LT.

which indicates the meta set constructed by hierarchical sampling has a more similar distribution to the test set.

**Effect of class-specific label corrector.** To valid the class-specific design of our label corrector, we build a class-agnostic variant and evaluate it on CIFAR-10-N with 40% asymmetric noise that holds different noise rates across different classes. The results show that our class-specific label corrector significantly outperforms its class-agnostic counterpart by a large margin of 4.0% in accuracy (94.51% vs. 90.56%), which clearly proves our class-specific design.

**Effect of meta net architecture.** To validate the architecture design of meta net, we simplify the label corrector and the margin generator to a  $R$ -length and a  $C$ -length learnable vector, respectively. Table 4 shows such modifications lead to a noticeable performance drop (0.27%). The explanation, which is supported by our experimental observation, is that MLPs learn proper label weights and per-class margins very quickly, while the learnable vectors, unfortunately, suffer from slow convergence.

**Test on different classifier.** To validate the generality of our method, we further evaluate it using the PAREs18. We respectively set the imbalance ratios and noise rates to  $\{10, 50, 100\}$  and  $\{0.2, 0.4\}$  and present the mean accuracy in Table 5. It shows our method also outperforms HAR on both CIFAR-10-N-LT and CIFAR-100-N-LT. This evidences our dynamic loss is applicable to various classifiers.

## Conclusions

This work presents a new dynamic loss for robust learning from long-tailed data with noisy labels. The dynamic loss comprises a learnable label corrector and margin generator, which is capable of jointly correcting noisy labels and adjusting classification margins to guide the learning of a classifier. The meta net and the classifier are co-optimized through meta-learning, thanks to a new hierarchical sampling strategy that helps provide unbiased yet diverse meta

data. Extensive evaluations on both synthetic and real-world data show our dynamic loss is effective and has high adaptability and robustness to various types of data biases.

## References

- Berthelot, D.; Carlini, N.; Goodfellow, I.; Papernot, N.; Oliver, A.; and Raffel, C. 2019. Mixmatch: A holistic approach to semi-supervised learning. In *NeurIPS*.
- Buda, M.; Maki, A.; and Mazurowski, M. A. 2018. A systematic study of the class imbalance problem in convolutional neural networks. *Neural Networks*, 106: 249–259.
- Cao, K.; Chen, Y.; Lu, J.; Arechiga, N.; Gaidon, A.; and Ma, T. 2020. Heteroskedastic and imbalanced deep learning with adaptive regularization. In *ICLR*.
- Cao, K.; Wei, C.; Gaidon, A.; Arechiga, N.; and Ma, T. 2019. Learning imbalanced datasets with label-distribution-aware margin loss. In *NeurIPS*.
- Chawla, N. V.; Bowyer, K. W.; Hall, L. O.; and Kegelmeyer, W. P. 2002. SMOTE: synthetic minority over-sampling technique. *Journal of artificial intelligence research*, 16: 321–357.
- Chen, M.; Cheng, H.; Du, Y.; Xu, M.; Jiang, W.; and Wang, C. 2021. Two Wrongs Don’t Make a Right: Combating Confirmation Bias in Learning with Label Noise. arXiv:2112.02960.
- Chen, W.; Zhu, C.; and Chen, Y. 2021. Sample Prior Guided Robust Model Learning to Suppress Noisy Labels. arXiv:2112.01197.
- Chen, Y.; Hu, S. X.; Shen, X.; Ai, C.; and Suykens, J. A. K. 2022. Compressing Features for Learning with Noisy Labels. *TNNLS*.
- Cubuk, E. D.; Zoph, B.; Mane, D.; Vasudevan, V.; and Le, Q. V. 2019. Autoaugment: Learning augmentation strategies from data. In *CVPR*.
- Cui, Y.; Jia, M.; Lin, T.-Y.; Song, Y.; and Belongie, S. 2019. Class-balanced loss based on effective number of samples. In *CVPR*.
- Deng, J.; Dong, W.; Socher, R.; Li, L.-J.; Li, K.; and Fei-Fei, L. 2009. Imagenet: A large-scale hierarchical image database. In *CVPR*.
- Engleson, E.; and Azizpour, H. 2021. Generalized jensen-shannon divergence loss for learning with noisy labels. In *NeurIPS*.
- Han, B.; Yao, Q.; Yu, X.; Niu, G.; Xu, M.; Hu, W.; Tsang, I.; and Sugiyama, M. 2018. Co-teaching: Robust training of deep neural networks with extremely noisy labels. In *NeurIPS*.
- He, K.; Zhang, X.; Ren, S.; and Sun, J. 2016a. Deep residual learning for image recognition. In *CVPR*.
- He, K.; Zhang, X.; Ren, S.; and Sun, J. 2016b. Identity mappings in deep residual networks. In *ECCV*.
- Huang, C.; Li, Y.; Loy, C. C.; and Tang, X. 2016. Learning deep representation for imbalanced classification. In *CVPR*.
- Huang, C.; Li, Y.; Loy, C. C.; and Tang, X. 2019a. Deep imbalanced learning for face recognition and attribute prediction. *TPAMI*, 42(11): 2781–2794.
- Huang, J.; Qu, L.; Jia, R.; and Zhao, B. 2019b. O2U-Net: A simple noisy label detection approach for deep neural networks. In *CVPR*.
- Huang, Y.; Bai, B.; Zhao, S.; Bai, K.; and Wang, F. 2022. Uncertainty-Aware Learning against Label Noise on Imbalanced Datasets. In *AAAI*.
- Jiang, L.; Zhou, Z.; Leung, T.; Li, L.-J.; and Fei-Fei, L. 2018. Mentornet: Learning data-driven curriculum for very deep neural networks on corrupted labels. In *ICML*.
- Jiang, S.; Li, J.; Wang, Y.; Huang, B.; Zhang, Z.; and Xu, T. 2022. Delving into Sample Loss Curve to Embrace Noisy and Imbalanced Data. In *AAAI*.
- Kang, B.; Xie, S.; Rohrbach, M.; Yan, Z.; Gordo, A.; Feng, J.; and Kalantidis, Y. 2019. Decoupling representation and classifier for long-tailed recognition. In *ICLR*.
- Kingma, D. P.; and Ba, J. 2015. Adam: A Method for Stochastic Optimization. In *ICLR*.
- Krizhevsky, A.; Hinton, G.; et al. 2009. Learning multiple layers of features from tiny images.
- Kumar, M. P.; Packer, B.; and Koller, D. 2010. Self-Paced Learning for Latent Variable Models. In *NeurIPS*.
- Li, J.; Socher, R.; and Hoi, S. C. 2020. Dividemix: Learning with noisy labels as semi-supervised learning. In *ICLR*.
- Li, W.; Wang, L.; Li, W.; Agustsson, E.; and Van Gool, L. 2017. Webvision database: Visual learning and understanding from web data. arXiv:1708.02862.
- Lin, T.-Y.; Goyal, P.; Girshick, R.; He, K.; and Dollár, P. 2017. Focal loss for dense object detection. In *ICCV*.
- Liu, S.; Niles-Weed, J.; Razavian, N.; and Fernandez-Granda, C. 2020. Early-learning regularization prevents memorization of noisy labels. In *NeurIPS*.
- Liu, Z.; Miao, Z.; Zhan, X.; Wang, J.; Gong, B.; and Yu, S. X. 2019. Large-scale long-tailed recognition in an open world. In *CVPR*.
- Loshchilov, I.; and Hutter, F. 2017. Sgdr: Stochastic gradient descent with warm restarts. In *ICLR*.
- Menon, A. K.; Jayasumana, S.; Rawat, A. S.; Jain, H.; Veit, A.; and Kumar, S. 2020. Long-tail learning via logit adjustment. arXiv:2007.07314.
- Reed, S.; Lee, H.; Anguelov, D.; Szegedy, C.; Erhan, D.; and Rabinovich, A. 2014. Training deep neural networks on noisy labels with bootstrapping. arXiv:1412.6596.
- Ren, J.; Yu, C.; Sheng, S.; Ma, X.; Zhao, H.; Yi, S.; and Li, H. 2020. Balanced meta-softmax for long-tailed visual recognition. In *NeurIPS*.
- Shu, J.; Xie, Q.; Yi, L.; Zhao, Q.; Zhou, S.; Xu, Z.; and Meng, D. 2019. Meta-weight-net: Learning an explicit mapping for sample weighting. In *NeurIPS*.
- Shu, J.; Yuan, X.; Meng, D.; and Xu, Z. 2022. CMW-Net: Learning a Class-Aware Sample Weighting Mapping for Robust Deep Learning. arXiv:2202.05613.
- Simonyan, K.; and Zisserman, A. 2015. Very Deep Convolutional Networks for Large-Scale Image Recognition. In *ICLR*.



Song, H.; Kim, M.; and Lee, J.-G. 2019. Selfie: Refurbishing unclean samples for robust deep learning. In *ICML*.

Szegedy, C.; Ioffe, S.; Vanhoucke, V.; and Alemi, A. A. 2017. Inception-v4, inception-resnet and the impact of residual connections on learning. In *AAAI*.

Tan, J.; Wang, C.; Li, B.; Li, Q.; Ouyang, W.; Yin, C.; and Yan, J. 2020. Equalization loss for long-tailed object recognition. In *CVPR*.

Tang, K.; Huang, J.; and Zhang, H. 2020. Long-tailed classification by keeping the good and removing the bad momentum causal effect. In *NeurIPS*.

Van der Maaten, L.; and Hinton, G. 2008. Visualizing data using t-SNE. *Journal of machine learning research*, 9(11).

Wei, T.; Shi, J.-X.; Tu, W.-W.; and Li, Y.-F. 2021. Robust long-tailed learning under label noise. arXiv:2108.11569.

Xu, Y.; Zhu, L.; Jiang, L.; and Yang, Y. 2021. Faster meta update strategy for noise-robust deep learning. In *CVPR*.

Zhang, Y.; Zheng, S.; Wu, P.; Goswami, M.; and Chen, C. 2021. Learning with Feature-Dependent Label Noise: A Progressive Approach. In *ICLR*.

---

**Algorithm 1: Robust learning with dynamic loss**


---

**Input:** training set  $\{(\mathbf{x}_i, \mathbf{y}_i)\}_{i=1}^N$ , learning rate  $\eta$ , number of warm-up iterations  $T_0$ .

// Warm-up Stage: run SGD for  $T_0$  iterations.

**for**  $t = 1, \dots, T_0$  **do**

Sample  $m_0$  examples  $\{(\mathbf{x}_i, \mathbf{y}_i)\}_{i=1}^{m_0}$  from  $\mathcal{D}$ .

$\mathbf{w}_{t+1} = \mathbf{w}_t - \eta_0 \bar{\mathbf{g}}_t$ , where  $\bar{\mathbf{g}}_t = \frac{1}{m_0} \sum_{i=1}^{m_0} \nabla \ell(\mathbf{w}_t; \mathbf{x}_i)$ .

// Robust Learning Stage: run SGD for  $T$  iterations.

**for**  $t = 1, \dots, T$  **do**

**if** New Epoch **then**

Compute rank  $r$  of samples.

Split set  $\mathcal{D}$  into a meta set  $\mathcal{D}_c$  and a train set  $\mathcal{D}_n$  by hierarchical sampling.

Optimize the  $\mathcal{G}_\theta$  via meta learning on dataset  $\mathcal{D}_c$  and  $\mathcal{D}_n$  as in Equation 7 and 8 in the manuscripts.

Update model parameters of classifier by our dynamic loss as in Equation 9 in the manuscripts.

---

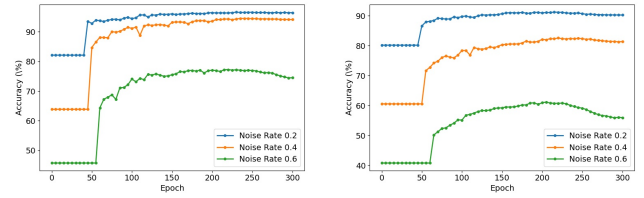


Figure 6: The visualization of the accuracy of generated label varied with epoch of  $\mathcal{G}_\theta$  on CIFAR-10-N (left) and CIFAR-100-N (right) with noise rates  $\lambda$  ranging from 0.2 to 0.6.

### Algorithm Pseudocode

Algorithm 1 depicts the detailed learning process. We begin by a warm-up stage to pre-train  $\mathbf{f}_\omega$  on the entire training set  $\mathcal{D}$  to possess preliminary classification capability. Then we enter a robust learning stage to optimize  $\mathcal{G}_\theta$  and  $\mathbf{f}_\omega$  in an alternative manner. Concretely, at the beginning of each epoch, we first construct a small meta set from  $\mathcal{D}$ , which is balanced and almost clean, by selecting samples with low classification loss value computed by the latest  $\mathbf{f}_\omega$ . The remaining samples of  $\mathcal{D}$  form a large counterpart set  $\mathcal{D}_n$ . Details of the optimization are presented in manuscripts. Source code is available at code [https://anonymous.4open.science/r/dynamic\\_loss-7BED](https://anonymous.4open.science/r/dynamic_loss-7BED). Since the hyperlink is forbidden, please copy and paste the URL. There may be some mistakes directly copying from PDF, please check it.

### Additional Visualizations

**CIFAR-N.** Figure 6 depicts the accuracy of corrected labels, computed as the proportion of samples with ground-truth labels after label correction. The label accuracy gradually increases as the training proceeds and the classifier becomes more trustworthy, and eventually reaches over 90% on CIFAR-10-N with noise rates 0.2 and 0.4. Notably, the accuracy also has been greatly improved by 35% under a

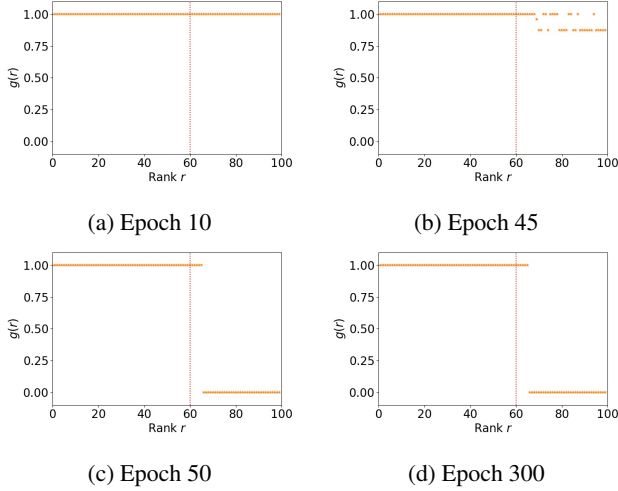


Figure 7: The visualization of learnable weight  $g(r)$  of class 1 varied with training epochs on CIFAR-10-N with noise rate  $\lambda = 0.4$ .

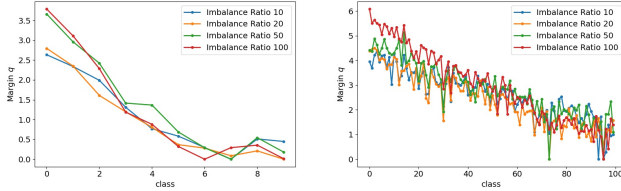


Figure 8: The visualization of the learned class-aware margin of  $G_L(\theta_L)$  on CIFAR-10-LT (left) and CIFAR-100-LT (right) with imbalance factor  $\rho$  ranging from 10 to 100.

noise rate of 0.6. The high accuracy of corrected labels validates our design choices from two perspectives: i) this supports our assumption that the classifier normally dedicates to fitting in the dominated clean samples, and can transfer the learned knowledge to noisy samples to predict the ground-truth labels for them; ii) the label corrector can accurately recognize noisy samples and correct their labels with the predicted correct ones.

Figure 7 shows the learnable weight varied with training epochs. From it we can know, at the beginning the label corrector tends to use the given label to train the classifier while it gradually changes to believe prediction label for the samples with large rank when the classifier is trained 45 epochs. Moreover, the label corrector accurately estimates the noise rate is about 35% (for noise rate 40%, there are actually 35% noisy samples). From this plot together with Figure 6, we find the epoch of label corrector believing the classifier is delayed as the noise rate increases. We believe the label corrector thinks the classifier needs to be trained more epochs to generate more reliable prediction labels as noise rate of train set increases. It evidences the label corrector can dynamically relabel the noisy labels according to the status of classifier and train set.

**CIFAR-LT.** Figure 8 visualizes the margins generated by

Datasets	Cross Entropy	AutoAugment	DivideMix	Balanced-Softmax	HAR	Ours
CIFAR-10	92.91	94.84	91.59	<b>94.95</b>	92.10	94.07
CIFAR-100	69.18	<b>73.96</b>	63.72	73.90	70.70	73.24

Table 6: Test accuracy (%) of ResNet32 on CIFAR datasets.

the margin generator under different imbalance ratios. One can see that despite of varying imbalance ratios, the generated margin consistently decays as the sample size grows (corresponding to increasing class index). Moreover, the learned margin variation across different classes tends to enlarge as the imbalance ratio increases. Both quantitative (in the manuscripts) and qualitative analyses evidence that the margin generator well respects and adapts to various class distributions by learning to assign proper margins automatically.

Figure 9 shows the classification margins and feature distributions of meta set varied with training epochs. From it we can know, the margin generator always adjusts the classification margins according to the feature distributions of meta set in the training process. Take the class 10 as an example, the margin generator tends to give a small classification margin to it since it is hard to recognise at the epoch 50. However, recognising it becomes easy at the epoch 250 and then the margin generator gives it a more large classification margin. It evidences the margin generator can dynamically adjust the classification margin according to classification difficulty.

**Webvision.** Considering the large number of categories in WebVision, we select 10 categories in intervals of 5 to visualize their learned label weights. As shown in Figure 10, the learned label weights are varied with different classes, suggesting the noise rates of different classes are different, which is consistent with real-world dataset. Moreover, the generated margins over different classes accord with the complex variation of sample size, as shown in Figure 11. This demonstrates our method adapts well to complicated real-world biased data.

**Animal-10N.** We also analyze the behavior of label corrector on real-word noisy data Animal-10N, as in Figure 12. Most of the learned label weight remains to be 1 and drops to 0 at around bin 92 (red dotted line), suggesting the noise rate estimated by the label corrector is about 8%, which is consistent with the well-recognized estimated noise rate on Animal-10N (Song, Kim, and Lee 2019).

**ImageNet-LT.** We also analyze the behavior of margin generator on long-tailed data ImageNet-LT, as in Figure 13. Considering the large number of categories in ImageNet-LT, we select 333 categories in intervals of 3 to visualize their learned margin. As shown in Figure 13, the learned margins are consistently varied with sample number of classes, suggesting the margin generator can generate proper margin for different classes.

## Test on unbiased dataset

Methods specially designed to cope with data bias may sometimes cause performance degradation on unbiased data. We evaluate different methods for robust learning on unbi-

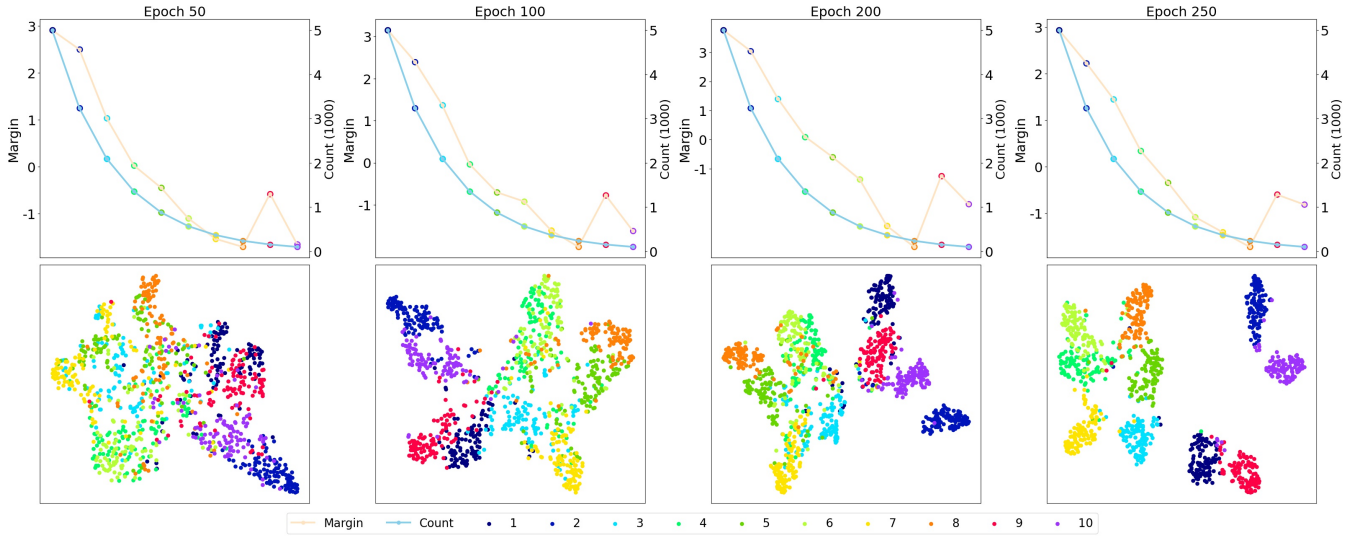


Figure 9: Visualization of learned classification margins and feature distributions of meta set varied with training epochs.

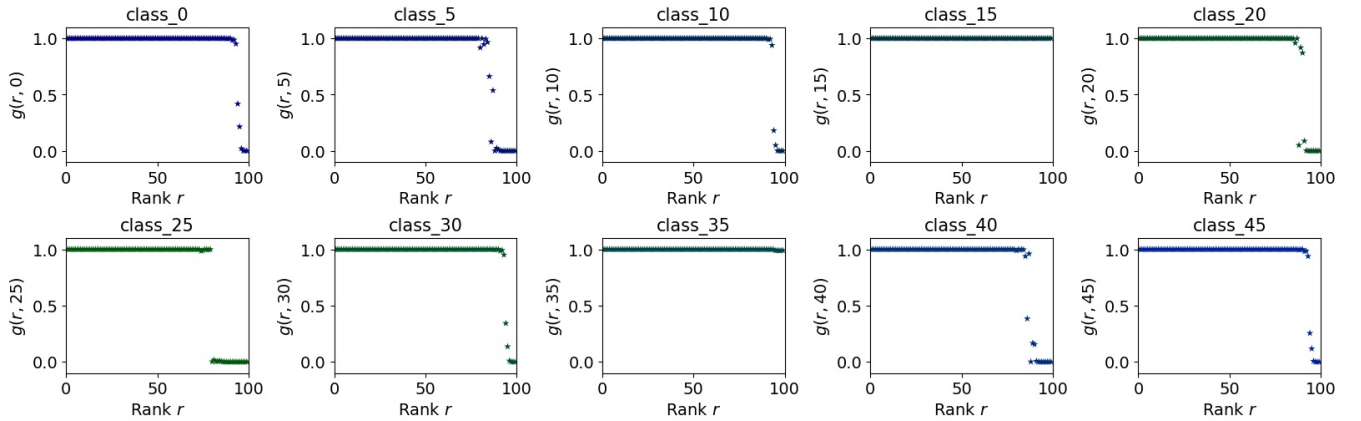


Figure 10: Visualization of per class learned label weights on WebVision.

used data. Table 6 shows some priors like DivideMix and HAR suffer noticeable accuracy drop, while our method still performs well on both CIFAR-10 and CIFAR-100. This shows our dynamic loss can adaptively set up proper learning objectives depending on the situations of training data.

### Training Time Analysis

Since the training time is the most concerned issues of meta learning, we also evaluate the total training time of our methods following DivideMix. Thanks to the solution to accelerate the training speed of meta learning by FaMUS (Xu et al. 2021) and CurveNet (Jiang et al. 2022), we train a model using about 7.2h with NVIDIA GTX 1080 ti, which is a little slower than DivideMix with Nvidia V100 GPU (5.2h). It evidences the efficiency of our method.

### Additional Dataset Details

**CIFAR.** Both of CIFAR-10 and CIFAR-100 consist of 60,000 RGB images (50,000 for training and 10,000 for test-

ing) and are equally distributed to 10 and 100 categories respectively.

**CIFAR-N.** CIFAR-N is simulated noisy data set based on CIFAR. Commonly simulated label noise types include symmetric and asymmetric noise. Symmetric noise is generated by randomly changing the labels with all possible labels according to a fixed probability of  $\lambda$  (noise rate). Asymmetric noise is manually designed to mimic the real-world label noise, where labels are only changed with those in similar classes such as deer  $\rightarrow$  horse and dog  $\leftrightarrow$  cat.

**CIFAR-LT.** CIFAR-LT is simulated long-tailed data set based on CIFAR, which reduces the number of training samples per class according to an exponential function  $n_i = n\mu^i$ . The  $i$ ,  $n_i$  and  $n$  is class index, the amount of samples of  $i$ -class and the maximum amount of samples in all classes.

**Webvision.** WebVision (Li et al. 2017) is a large-scale real-world dataset with both label noise and class imbalance. It contains 2.4 million images among which about 20% are mislabeled (Chen et al. 2021). Following MentorNet (Jiang

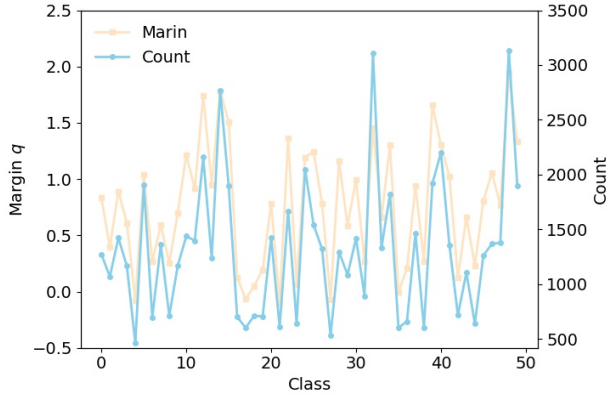


Figure 11: Visualization of learned per-class margins on Webvision.

Datasets		CIFAR-10	CIFAR-100	Webvision	Animal-10N	ImageNet-LT
Classifier	Optimizer	SGD				
	Momentum	0.9				
	Weight Decay	5.00e-04	5.00e-04	1.00e-4	5.00E-04	1.00e-4
	Learning rate	0.1	0.1	0.02	0.02	0.1
	Learning scheduler	Cosine Annealing				
MetaNet	Optimizer	Adam				
	Weight Decay	0				
	Learning rate	3.00e-03				
	Learning scheduler	Fixed				
Others	M0	0.5	0.5	0.5	0.5	-
	M1	0.25	0.25	0.25	0.25	-
	Epoch	300	300	150	100	90
	Warmup Epoch	5	5	1	5	0
	Batch Size	512	512	64	128	128
	Rank Number	100	50	100	100	-

Table 7: Additional Training Details

et al. 2018), we create the miniWebVision dataset by selecting the images of top 50 classes, with an observed imbalance ratio of about 6.78. We test the model on the val set of WebVision and ImageNet (Deng et al. 2009).

**Animal-10N.** ANIMAL-10N dataset contains 5 pairs of confusing animals with a total of 55,000 images (50,000 for training and 5,000 for testing), and they are equally distributed to all categories. These images are crawled from website with the given labels as the search keyword, which inevitably has a lot of noise. The noise rate is estimated to be around 8%.

**ImageNet-LT.** The ImageNet-LT contains 115.8K images distributed to 1,000 categories according to Pareto distribution, where the amount of images per class ranges from 5 to 1280.

### Additional Training Details

All of the training details are presented in Table 7. For the meta net, we adopt the same setting for its generalizations. Adam optimizer (Kingma and Ba 2015) with a fixed learning rate 3e-3 and a weight decay of 0 is employed.

**CIFAR.** For CIFAR, we follow balanced-softmax to train all the classifier for 300 epochs with batch size 512. The learning rate is initialized as 0.1 and controlled by cosine annealing learning scheduler (Loshchilov and Hutter 2017). We train all classifiers with the same SGD optimizer for 300 epochs with a momentum of 0.9 and a weight decay of 5e-4. Following balanced-softmax, the RandomCrop, Random-Flip, AutoAugment are adopted for data augmentation. For fair comparison, we adopt the same data augmentation as in AutoAugment (Cubuk et al. 2019) to all these methods except for CurveNet (Jiang et al. 2022) due to incompatibility.

**Webvision.** We train the Inception-ResNet V2 for 150 epochs using SGD optimizer with momentum 0.9 and weight decay 1e-4. The number of epochs for the warm-up stage is 1 and the bath size is 64. The learning rate is initialized as 0.02 and controlled by cosine annealing learning scheduler.

**Animal-10N.** We train the VGG10-BN for 100 epochs using SGD optimizer with momentum 0.9 and weight decay 5e-4. The number of epochs for the warm-up stage is 5 and the bath size is 128. The learning rate is initialized as 0.02 and controlled by cosine annealing learning scheduler.

**ImageNet-LT.** Following previous works (Liu et al. 2019), we train the ResNet-10 for 90 epochs using SGD optimizer with momentum 0.9 and weight decay 1e-4. The number of epochs for the warm-up stage is 0 and the bath size is 128. The learning rate is initialized as 0.1 and controlled by cosine annealing learning scheduler.

### Detailed Results

Here we provide the detailed accuracy of all the settings. Tables 8 and 9 correspond to the CIFAR-10-N-LT and CIFAR-100-N-LT in Table 1 in manuscript. As shown in them, the performance of our last model is generally very close to that of our best model despite of varying bias settings. In contrast, the last models of DivideMix and Balanced-Softmax degrade significantly compared with their corresponding best models, especially on CIFAR-10 with severe imbalance and noise (e.g.,  $\rho = 100$  and  $\lambda = 0.5$ ). This indicates our method is much more resistant to overfitting on biased data than other methods.

Tables 10, 11, 12 and 13 correspond to Tables 2, 3, 4 and 5 in manuscript respectively.

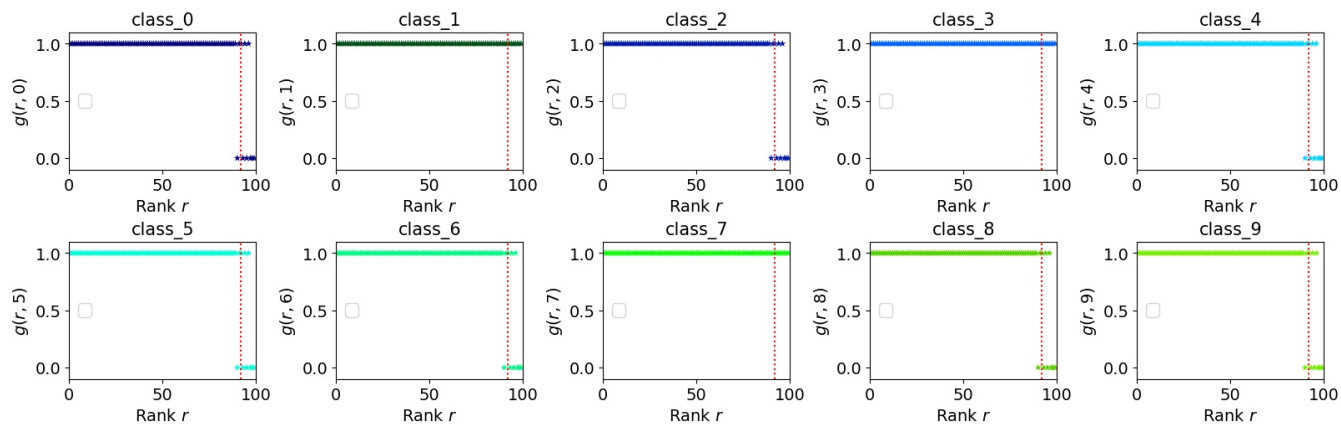


Figure 12: Visualization of per class learned label weights on Animal-10N.

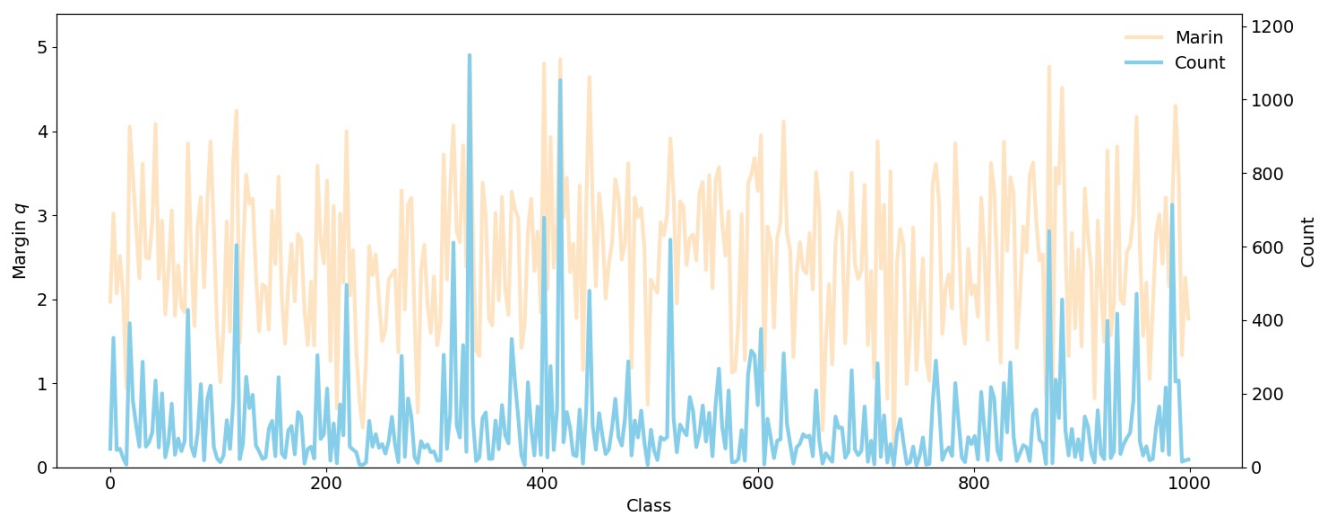


Figure 13: Visualization of learned class margins on ImageNet-LT.



Imbalance Ratio		10					100					Average
Noise Rate		0.1	0.2	0.3	0.4	0.5	0.1	0.2	0.3	0.4	0.5	
Cross Entropy	Last	76.63	68.89	61.21	54.01	44.09	59.99	50.56	44.81	37.13	30.02	52.73
	Best	77.14	74.35	72.22	68.28	59.65	63.45	53.45	49.49	45.53	40.76	60.43
DivideMix	Last	88.11	86.95	66.42	73.78	73.85	63.08	61.14	24.31	24.13	20.09	58.19
	Best	88.50	87.13	67.67	74.26	74.15	63.08	61.61	33.79	31.06	26.10	60.74
Balanced-Softmax	Last	87.52	84.00	79.49	73.53	65.27	76.14	69.37	62.03	52.79	46.44	69.66
	Best	87.62	84.50	82.84	79.09	75.90	78.63	73.29	70.89	67.57	63.40	76.37
DivideMix +Balanced-Softmax	Last	88.23	86.96	78.02	79.17	76.89	76.63	75.72	46.82	53.25	54.33	71.60
	Best	<b>88.93</b>	86.06	79.19	79.81	78.20	79.36	76.55	48.60	54.99	55.84	72.75
CurveNet	Last	84.10	81.70	78.47	78.73	75.65	65.77	66.21	62.37	48.71	51.85	69.36
	Best	84.87	84.62	79.98	81.33	78.37	67.55	68.72	63.71	51.63	52.84	71.36
HAR	Last	86.46	84.27	81.78	79.55	78.07	<b>78.60</b>	75.05	72.08	65.48	63.90	76.52
	Best	87.03	84.47	81.94	79.87	78.25	<b>79.02</b>	76.14	72.74	67.22	65.00	77.17
FaMUS	Last	65.94	43.73	56.10	52.75	69.79	23.42	26.20	22.50	18.46	12.27	39.12
	Best	68.82	52.28	59.10	53.48	73.01	34.09	37.55	32.23	30.26	28.98	46.98
ELR+	Last	85.21	85.71	84.13	81.16	78.91	64.76	61.41	56.42	51.31	44.05	69.31
	Best	87.04	86.14	84.38	83.30	80.23	65.73	62.12	56.42	52.26	45.73	70.34
Ours	Last	<b>89.23</b>	<b>88.39</b>	<b>86.58</b>	<b>84.43</b>	<b>83.34</b>	77.80	<b>76.31</b>	<b>74.10</b>	<b>69.64</b>	<b>67.45</b>	<b>79.73</b>
	Best	<b>89.44</b>	<b>88.46</b>	<b>86.72</b>	<b>84.73</b>	<b>83.71</b>	78.96	<b>76.64</b>	<b>76.17</b>	<b>70.37</b>	<b>70.26</b>	<b>80.55</b>

Table 8: Detailed Test accuracy (%) on CIFAR-10-N-LT with varying imbalance and noise.

Imbalance Ratio		10					100					Average
Noise Rate		0.1	0.2	0.3	0.4	0.5	0.1	0.2	0.3	0.4	0.5	
Cross Entropy	Last	43.48	37.25	31.34	25.53	19.45	29.92	21.85	19.32	13.71	12.21	25.41
	Best	43.95	37.64	32.18	29.44	23.87	30.52	22.13	19.58	14.59	12.81	26.67
DivideMix	Last	54.17	51.92	50.44	45.02	43.43	36.31	35.68	34.10	33.19	27.22	41.15
	Best	54.94	53.35	50.93	45.36	43.44	36.99	36.24	34.87	33.64	27.74	41.75
Balanced-Softmax	Last	58.38	54.59	50.49	44.83	40.45	43.17	38.67	33.27	27.08	22.10	41.30
	Best	58.62	54.73	50.66	45.63	40.56	43.50	38.67	33.62	28.05	24.19	41.82
DivideMix +Balanced-Softmax	Last	56.37	54.80	54.83	51.29	48.89	43.26	42.42	40.46	37.83	30.95	46.11
	Best	56.85	56.06	55.64	52.30	50.01	43.67	42.79	40.99	38.50	32.38	46.92
CurveNet	Last	50.41	47.14	43.18	41.23	34.85	22.10	20.44	17.80	11.87	9.24	29.83
	Best	52.73	51.93	47.56	44.08	39.74	25.26	21.35	18.72	13.60	12.20	32.72
HAR	Last	58.88	55.43	52.57	46.01	43.96	42.67	39.39	34.43	29.43	24.94	42.77
	Best	59.32	55.80	53.44	46.75	44.61	44.45	40.98	36.09	31.17	27.15	43.98
FaMUS	Last	46.07	51.59	46.07	46.93	43.83	29.33	30.22	28.53	27.83	24.57	30.72
	Best	47.03	52.05	46.41	47.88	44.30	29.66	30.31	28.50	27.24	24.85	30.81
ELR+	Last	52.48	51.30	46.24	39.98	34.91	33.01	28.10	24.92	22.11	16.54	34.96
	Best	53.91	51.90	47.88	42.61	37.35	33.81	28.94	26.10	22.11	17.39	36.20
Ours	Last	<b>59.24</b>	<b>57.57</b>	<b>56.85</b>	<b>52.07</b>	<b>50.74</b>	<b>47.23</b>	<b>45.74</b>	<b>42.72</b>	<b>39.58</b>	<b>33.87</b>	<b>48.56</b>
	Best	<b>59.52</b>	<b>57.85</b>	<b>57.32</b>	<b>52.66</b>	<b>51.26</b>	<b>47.55</b>	<b>45.82</b>	<b>43.54</b>	<b>39.96</b>	<b>34.30</b>	<b>48.98</b>

Table 9: Detailed Test accuracy (%) on CIFAR-100-N-LT with varying imbalance and noise.

Datasets	Cifar-10						Cifar-100			
Noise Rate	20	40	60	20(Asym.)	40(Asym.)	Average	20	40	60	Average
CE	86.98	77.52	73.63	83.60	77.85	79.92	60.38	46.92	31.82	46.37
SELFIE	86.39	82.23	74.81	-	-	-	55.71	51.14	43.85	50.23
PLC	86.40	71.72	65.22	90.23	85.40	79.79	59.66	49.24	33.18	47.36
NCT	95.00	87.00	73.22	91.51	93.00	87.95	67.65	57.97	45.01	56.88
Coteaching	93.83	91.74	57.65	93.23	90.78	85.45	70.81	62.65	41.55	58.34
CMW-Net	91.09	86.91	83.33	93.02	92.70	89.41	70.11	65.84	56.93	64.29
DivdeMix	95.63	93.78	<b>94.23</b>	94.18	92.73	94.11	77.20	73.37	<b>70.75</b>	73.77
GJS	94.20	92.80	89.72	91.92	86.07	90.94	73.31	71.33	66.92	70.52
Ours	<b>95.90</b>	<b>94.69</b>	92.28	<b>95.74</b>	<b>94.51</b>	<b>94.62</b>	<b>78.26</b>	<b>75.28</b>	69.18	<b>74.24</b>

Table 10: Detailed accuracy (%) of PAREs18 on CIFAR-N with different settings.

Datasets	Cifar-10-LT					Cifar-100-LT				
Imbalance Ratio	10	20	50	100	Average	10	20	50	100	Average
CE LOSS	86.39	82.23	74.81	70.36	78.45	55.71	51.14	43.85	38.32	47.26
Focal Loss	86.66	82.76	76.71	70.38	79.13	55.78	51.95	44.32	38.41	47.62
CB Focal	87.49	84.36	79.27	74.57	81.42	57.99	52.59	45.32	39.6	48.88
LDAM-DRW	87.68	85.51	81.64	78.02	83.21	44.7	52.93	48.22	59.59	51.36
FaMUS	87.9	86.24	83.32	80.96	84.61	59	55.95	49.93	46.03	52.73
Balanced-Softmax	91.01	<b>88.85</b>	86.44	82.31	87.15	<b>64.00</b>	59.48	54.36	<b>50.47</b>	57.08
Ours	<b>91.24</b>	88.30	<b>86.46</b>	<b>82.95</b>	<b>87.24</b>	63.99	<b>59.79</b>	<b>54.51</b>	50.14	<b>57.11</b>

Table 11: Detailed accuracy (%) of ResNet on CIFAR-LT with different settings.

$\mathcal{G}_{\theta_l}$	$\mathcal{G}_{\theta_m}$	B	H	V	Imbalance Ratio	10					100					Average
					Noise Rate	0.1	0.2	0.3	0.4	0.5	0.1	0.2	0.3	0.4	0.5	
					Last	76.63	68.89	61.21	54.01	44.09	59.99	50.56	44.81	37.13	30.02	52.73
					Best	77.14	74.35	72.22	68.28	59.65	63.45	53.45	49.49	45.53	40.76	60.43
	✓			✓	Last	88.15	86.16	82.86	80.84	65.36	74.52	67.71	63.71	54.28	51.47	71.51
					Best	88.37	86.37	83.39	81.88	75.70	77.08	72.80	71.67	67.67	63.46	76.84
✓				✓	Last	88.39	86.00	83.46	81.04	74.71	73.33	50.99	63.23	56.79	52.82	71.08
					Best	88.51	86.15	83.90	82.01	77.68	76.49	71.28	71.03	68.04	66.05	77.11
✓		✓	✓		Last	85.72	81.79	82.27	81.62	69.36	78.93	72.11	71.36	51.16	52.11	72.64
					Best	87.61	82.44	83.05	82.28	69.81	79.64	73.27	71.85	59.65	59.98	74.96
✓	✓				Last	87.46	85.86	83.85	83.68	77.58	<b>79.43</b>	<b>76.49</b>	73.55	<b>70.72</b>	66.65	78.53
					Best	87.79	86.24	84.77	83.91	78.08	<b>80.44</b>	<b>77.91</b>	75.13	<b>72.56</b>	68.92	79.58
✓	✓		✓	✓	Last	<b>88.65</b>	86.88	85.72	85.32	81.68	78.42	76.38	74.59	68.42	68.98	79.50
					Best	89.06	87.18	86.00	<b>85.41</b>	82.06	79.35	77.36	75.46	71.51	70.13	80.35
✓	✓		✓		Last	88.32	<b>87.08</b>	<b>85.74</b>	<b>85.42</b>	<b>83.39</b>	78.25	74.89	<b>75.48</b>	69.92	<b>69.17</b>	<b>79.77</b>
					Best	<b>89.44</b>	<b>88.46</b>	<b>86.72</b>	84.73	<b>83.71</b>	78.96	76.64	<b>76.17</b>	70.37	<b>70.26</b>	<b>80.55</b>

Table 12: Detailed accuracy (%) of ablations on CIFAR-10-N-LT with different settings .

Datasets		Cifar-10-N-LT							Cifar-100-N-LT						
Imbalance Ratio		10		50		100		Average	10		50		100		Average
Noise Rate		0.2	0.4	0.2	0.4	0.2	0.4		0.2	0.4	0.2	0.4	0.2	0.4	
HAR	Last	84.49	68.22	81.64	63.15	70.95	58.09	71.09	53.02	44.68	43.18	28.15	38.94	28.15	39.35
	Best	84.70	68.88	82.56	63.84	71.12	58.68	71.63	53.45	45.44	43.74	28.59	39.37	28.59	39.86
Ours	Last	<b>90.06</b>	<b>87.20</b>	<b>82.41</b>	<b>76.08</b>	<b>74.41</b>	<b>69.80</b>	<b>79.99</b>	<b>54.53</b>	<b>45.01</b>	<b>44.19</b>	<b>32.26</b>	<b>40.50</b>	<b>30.43</b>	<b>41.15</b>
	Best	<b>90.23</b>	<b>87.57</b>	<b>83.74</b>	<b>79.21</b>	<b>78.63</b>	<b>73.79</b>	<b>82.20</b>	<b>55.04</b>	<b>46.64</b>	<b>44.63</b>	<b>32.75</b>	<b>40.58</b>	<b>30.76</b>	<b>41.73</b>

Table 13: Detailed accuracy (%) of PAREs18 on CIFAR-N-LT with different settings.